Entanglement Network Model Relating Tensile Impact Strength and the Ductile-Brittle Transition to Molecular Structure in Amorphous Polymers

B. H. BERSTED, *Research and Development Department, Amoco Chemicals Corporation, Amoco Research Center, Naperville, Illinois 60540*

Synopsis

A model is presented to account for the large variations in tensile and tensile impact strength of amorphous polymers from a consideration of an idealized entanglement network. The material strength under tensile impact conditions is shown to be predictable and to increase with the "fineness" of the entanglement network; a higher entanglement density leading to more molecular chains supporting the stress. The entanglement density is, in turn, shown to increase with number-average molecular weight and the quotient of the length to the molecular weight of the chemical repeat unit (empirically found to be related to the critical enganglement molecular weight). Ductile behavior is demonstrated to occur under tensile impact conditions when the material strength σ_B exceeds the yield stress σ_y and brittle behavior when $\sigma_y > \sigma_B$. It is further demonstrated that the large variation in tensile impact strength among the amorphous polymers studied can be adequately accounted for in terms of the large and predictable variation in σ_B; the larger σ_B is relative to σ_y, the more the polymer can draw (absorbing energy in the process) until σ_B is reached. Surprisingly, the predictions of strength for high-molecular-weight polycrystalline materials also gave good agreement with experimental data.

INTRODUCTION

The impact strength of polymers is a complex function of stress state, rate of deformation, temperature, molecular structure, and molecular weight. Generally, good impact strength is thought to arise out of the ability of a material to undergo yielding before a critical fracture stress is reached [Ludwik- Davidenov-Orowan (LDO) hypothesis,[1] see Fig. 1]. The ability to yield at stresses appreciably below the fracture stress is in turn thought to be due to molecular mobility under the particular test conditions (temperature, rate of testing, and sample configuration). Yielding and the resulting necking in the tensile mode dissipate large amounts of energy leading to good tensile impact strength (TIS). Therefore, predictions of ductile or brittle behavior in terms of the interplay between the yield and fracture stresses go a long way toward the understanding of TIS.

One approach, that was suggested[2] as early as 1959, is the study of molecular motion below the glass-transition temperature T_g; dynamic relaxation peaks should be present below the testing temperature for good impact properties. The position that impact strength (and chain mobility) is directly related to low-temperature "secondary" glass transitions has been discussed at some length by Sauer.[3] More recently, Yeh and Wyzoski[4] have shown that the embrittlement of polycarbonate upon annealing was not accompanied by changes in relaxation behavior.

Journal of Applied Polymer Science, Vol. 24, 37–50 (1979)

0021-8995/79/0024-0037$01.00

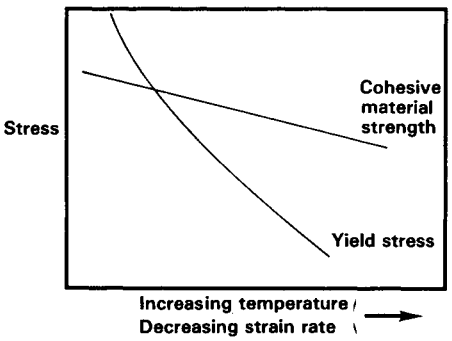

Fig. 1. Schematic diagram illustrating the Ludwik-Davidenov-Orowan theories of ductile-brittle transitions for temperatures below T_g or T_m (where the breaking stress falls to zero).

Additionally, it has been shown[5] that poly(phenylene oxide) is somewhat tougher than crystal polystyrene, even though no peaks can be detected between room temperature and liquid-nitrogen temperature. Furthermore, copolymers of methyl and cyclohexylmethacrylates show[5] a pronounced low-temperature peak and are extremely brittle at room temperature. The rationalization of these phenomena is the requirement that the low-temperature peak must be an "effective backbone motion" in order to provide good impact strength.

A different approach has been put forth by Bueche et al.[6] in which they assume that the maximum elongation to break for polystyrene and poly(methyl methacrylate) is accounted for by the elongation of the chains between entanglements (with no entanglement slippage). That there must be an element of truth in this approach is evident from the observations[7,8] that a large part of the deformation is recoverable if sufficient molecular mobility is effected; this behavior suggests a long-range interconnectiveness such as a rubberlike material with high internal viscosity, although this view is no doubt a gross oversimplification of a complex phenomenon.

Much attention has been focused on the yield behavior of polymers in various states of stress. Surprisingly, however, a much smaller effort has been directed toward the material strength, which according to the "LDO" hypothesis is equally important in the impact behavior. The present study will demonstrate that the very large variations in the TIS and the ductile-brittle transition can, in large part, be accounted for by a consideration of the intrinsic strength of an entanglement network structure. A model will be presented that is based on an assumed network in the amorphous polymer, in which the ultimate strength in tension is that of the interconnecting molecular strands spanning entanglement points.

EXPERIMENTAL

The samples used in this study are listed in Table I. The polycarbonate samples, polysulfone, polyphenylene oxide, polystyrene (sample K), poly(vinyl chloride), poly(ethyl methacrylate), and poly(vinyl acetate) were obtained from Aldrich Chemical Company as secondary standards with known molecular weight distributions. The remaining samples were produced by various commercial and experimental processes.

TABLE I
Comparison of Experimental and Predicted Failure Properties for Various Polymers

Sample ID	M_c ($\sim 2M_e$)	$\overline{M}_n$	$[\eta]$	σ_B (Predicted psi)	σ_B (Experimental)	ρ (g/cm^3)	l^* (cm)	Yield stress σ_y (psi)	Nominal drawing stress (σ_d)	TIS predicted (ft lb./in.^{2})	TIS experimental (ft lb/in.^{2})
Polycarbonate	4800					1.18					
Sample A		18,100		15,400	16,300		1.20	9075	9000	251	401 ± 88
Sample B		14,400		14,300	15,000		1.18	8300	8000	244	349 ± 130
Sample C		13,400		13,800	15,100		1.15	9600	8700	192	343 ± 113
Polysulfone	6300[a]	20,400		13,100	15,100	1.29	0.63	9880	7160	123	218 ± 36
Poly(ethylene terephthalate)	4500[a]										
Sample D		52,000	1.27	21,400	21,000	1.34	0.50	11,500	10,500	179	315 ± 7
Sample E		27,000	0.79	19,800	21,000	1.34	0.40	12,000	11,000		147 ± 18
Sample F		15,800	0.53	15,900	12,600	1.34	0.40	10,200	10,200		69 ± 37
Sample G		7600	0.31	10,900	1200	1.34		1200	—		16 ± 5
Poly(paramethylene benzoate) PPMB	5500[a]										
Sample H		21,300[b]	0.57	14,800	12,300	1.30	0.60	10,400	6200	169	203 ± 65
Sample I		8800[b]	0.30	8400	8000	1.30	—	—	—		19
Polyphenylene oxide	9000[a]	24,000		7100	9200(14,400)	1.05	—	—	—		37 ± 9 (240)
Poly(methyl methacrylate) (PMMA)	27,500	33,200	0.46	1040	4200	1.19	—	—	—		55 ± 7
Poly(ethyl methacrylate)	37,500[a]	144,000		2600	4050	1.09					6 ± 3
Polystyrene											
Sample J	31,200	42,000		1300	1800	1.04	—	—	—		22 ± 4
Sample K		84,600		2600	1860						
PEM_2 (Dimethyl-2,2′,6,6′ tetramethyl-biphenyl-4,4′ dicarboxylate)	7000[a]	16,400[b]	0.60	9500	7000	1.26	—	—	—		28 ± 2
UHMWPE, Ultrahigh molecular weight polyethylene	3800	c	7.9	19,800	24,000	0.92	1.25	4500	3800	656	1134
Poly(vinyl chloride)	7500[a]	24,400		11,300	8210	1.37					
Poly(vinyl acetate)	24,500	47,700		2900	2500	1.16					

[a] M_c estimated from Figure 4.
[b] $\overline{M}_n$ as determined from end group analysis.
[c] $\overline{M}_n$ assumed $\gg M_c$.

All specimens were tested for tensile impact using ASTM Type-L tensile bars, which were obtained from compression molded plaques (ASTM Designation D1822-61T). All compression molded samples were hard quenched in ice water to produce amorphous specimens. This was particularly hard to do for the lower-molecular-weight poly(ethylene terephthalate) (PET) samples. After the hard quenching no crystallinity by x ray could be detected (ca. 5% lower detection limit). Ductile specimens were cut out of the plaque using our die cutter, and brittle specimens were routed to the desired Type-L specimens.

The load-time curves were measured by the use of a strain gauge on the Charpy pendulum impact equipment. The strain gauge was adapted to measure load, and was calibrated using a calibrated force gauge. The resulting load-time trace was recorded on a Tektronix dual trace oscilloscope. A typical trace is shown in Figure 2 for a ductile specimen. The breaking stress was calculated as the load at break divided by the cross-sectional area of the specimen after break.

The low-temperature results reported here were produced by immersing the specimen and holder in liquid nitrogen, and quickly transferring it to the impact apparatus for breaking. The transfer took about 3–5 sec before breaking.

THEORY

The data presented by Berry[9] have shown that the surface energy (γ_s, the energy required to produce unit area of new surface), and therefore the tensile strength, tend toward zero as the molecular weight of the sample approaches a characteristic molecular weight (25,000) for poly(methyl methacrylate) (PMMA). This characteristic molecular weight is quite close to the critical molecular weight for entanglement for PMMA [ca. 27,500 (ref. 10)]. This result, together with similar results observed for polystyrene, suggest that the strength of amorphous polymers is related to the long-range interconnectiveness of an entanglement network. This view is further supported by the ability[7] of highly deformed amorphous polymers to recover to their original shape upon heating above the glass-transition temperature. This recovery suggests that amorphous polymers should be regarded as rubberlike materials with very high internal viscosities below their T_g.

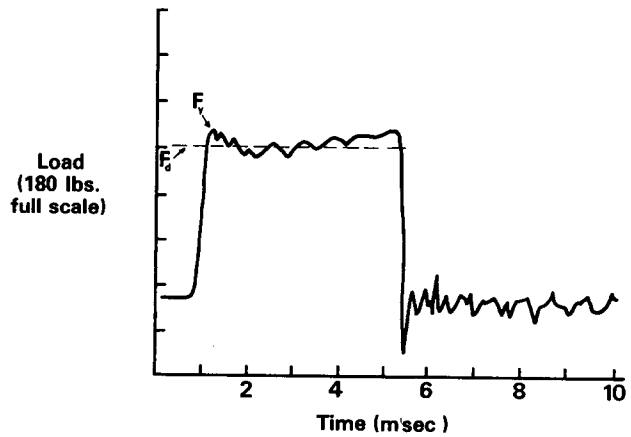

Fig. 2. Typical load-time oscilloscope trace for impact of the ductile polycarbonate (sample A) at 21°C. F_y is the load at yield and F_d the drawing load.

From the above ideas, it will be assumed as an integral part of the model to be developed that the true breaking stress in tension is the result of the interconnectiveness of an entanglement network. Van der Wals forces will be neglected in favor of the much stronger covalent bonds forming the entanglement network.

According to the LDO hypothesis,[1] the breaking stress depends little on strain, strain rate, and temperature, in marked contrast to the tensile yield stress; the process of yield and failure are considered independent processes. Figure 1 schematically demonstrates this point. The experimental data of Vincent[11] tend to confirm this trend. This relative insensitivity to temperature and test rate suggests that the breaking strength is a property of the material, which is to a first approximation independent of viscoelastic effects. Therefore, as our first approximation to the strength of amorphous polymers a hypothetical reference state will be chosen. This hypothetical ideal glassy reference state will be one in which no shear yielding can take place, but rather only normal stress failure. Upon application and subsequent rise of the stress, bonds (Van der Wals) are broken until the covalent bonds of a supporting chain is reached, with the result that small fissures may be imagined to develop throughout the sample with supporting interentanglement chains in the tensile direction blocking the growth of these fissures as schematically illustrated in Figure 3. The sample integrity is thus dependent on whether cracks between the supporting chains can grow. At the point of break these short interconnecting chain segments must be highly strained—their contributions to the macroscopic modulus being of the order of extended chains. This is not to imply that in the entanglement network the interentanglement molecular chains are fully extended, but rather that small segments spanning the fissures are highly strained.

The key postulate of the model is that at a given temperature T and elongational strain rate $\dot{\epsilon}$ the breaking stress of both brittle and ductile amorphous materials are represented, to within a multiplicative constant $K(T,\dot{\epsilon})$ (which depends on T and $\dot{\epsilon}$), by the breaking stress of the hypothetical glassy reference state. If we assume that the ideal glassy state is approximated by low temperature tensile data, the breaking stress (σ_B) for the immobilized reference state might be expected to be of the order of twice that at room temperature from the study of σ_B versus temperature by Vincent[11] and 2½ times from the data of Berry.[12] We therefore expect $K(T,\dot{\epsilon})$ to be ca. ½ at room temperature.

The plan is to attempt to calculate the strength of an entanglement network, in which no plastic flow takes place. The strength of this idealized state will,

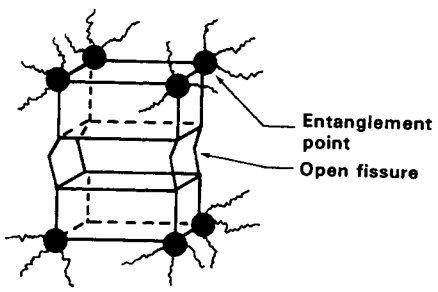

Fig. 3. Schematic model of the idealized entanglement structure after application of a tensile stress.

using the above assumption, be used to represent the breaking strength of the real material at room temperature. Admittedly, this assumption does not directly appear to take into account the complicated processes of crack growth, plastic flow, crazing, and craze fracture that no doubt take place prior to failure. However, some experimental data[11] tend to support my assumption. In the next section, polycarbonate, polysulfone, and poly(ethylene terephthalate) samples at room and low temperature, where ductile and brittle failures, respectively, occur, will be shown to have essentially the same values of σ_B (the true stress). Finally, the extent of agreement of predictions using this assumption with experimental findings will be taken as evidence of the essential correctness of the above postulate as a useful approximation.

From the above discussion it is evident that the strength of the material will be related to the number of supporting strands or interconnections in the tetrahedral entanglement network. For the case we are interested in here (impact conditions) we shall assume the entanglement junctions to behave as crosslinks with no slippage. Therefore, as Bueche[13] has done for relating tensile strengths of rubbers by using a three dimensional idealized network of crosslinked chains, we will make use of the following relationship of Bueche[13] to calculate the number of effective supporting chains per unit area n^2 in a given direction (taken to be the tensile direction here):

$$n^2 = [(2N_0\rho/3M_c)(1 - M_c/\overline{M}_n)]^{2/3} \tag{1}$$

N_0 is Avogadro's number, ρ is the sample density, M_c is equal to twice the molecular weight between entanglements (M_e), and $\overline{M}_n$ is the number-average molecular weight of the sample. From this point on, it will be tacitly assumed that $M_c = 2M_e$, although there is disagreement[10] on the exact relationship.

In general we may expect that the "finer" the entanglement network, the more molecular chains support the load and the higher the ultimate material strength, based on the instantaneous sample cross-sectional area, not the original cross-sectional area. In order to fabricate a relationship between the true breaking stress and the entanglement structure, the result of Orowan[14,15] for the rupture of a plane of atoms will be used. The relation of Orowan assumes the force-deflection relation of the strained localized elements is approximately sinusoidal and the radius of curvature of the crack tip is approximately the interatomic distance. Orowan's final result is

$$\sigma_B = (E\gamma_s/c)^{1/2}/2 \tag{2}$$

where $2c$ is the initial crack or fissure spacing (in our case will be $1/n$), γ_s is the energy required to create unit area of new surface, σ_B the applied stress at break, and E is the Young's modulus of the assembly of bridging chain segments across a plane as shown in Figure 3. As schematically indicated in Figure 3, upon application of the tensile stress, cracks form with a length of $1/n$ and widths corresponding to a couple of covalently bonded units. The assumption will be made that this intrinsic flaw due to the supermolecular structure is the most serious flaw in the specimen. Voids due to free volume distribution and other cavities originally present would not generally be expected to develop as high local stresses at the flaw tip as the interentanglement flaws envisioned because of the much smaller radius of curvature (sharper) of the postulated intrinsic flaws. The relative sharpness of the interentanglement fissures arises out of the assumed

lack of mobility in the reference state; chain segments would have to slide past each other in order to widen the crack width more than a couple of chain segments. In our case we will have

$$\gamma_s = E_B n^2/2N_0, \qquad E = n^2 E_0 A_0 \tag{3}$$

where E_B is the breaking energy per mole of bonds, E_0 is the crystal lattice modulus in the chain direction, and A_0 is the cross-sectional area of a lattice chain. Taking $2c = 1/n$, combining eqs. (1)–(3), and taking K to be the ratio between σ_B under the desired condition to be predicted and σ_B in the hypothetical reference state, we get

$$\sigma_B = \frac{K(T,\dot{\epsilon})}{2}\left(\frac{2}{3}\right)^{5/6}(N_0)^{1/3}(E_0A_0E_B)^{1/2}\left(\frac{\rho(1 - M_c/\overline{M}_n)}{M_c}\right)^{5/6} \tag{4}$$

Taking E_B to be 80 kcal/mole (very close[16] to either the carbon-carbon or carbon-oxygen covalent bond dissociation energy), E_0A_0 as 3.62×10^{-3} dyn [from the average of polyethylene and poly(ethylene terephthalate) values from x-ray measurements],[17] and K (297°K) $\simeq$ 1/2.35, we get

$$\sigma_B \text{ (psi)} = 2 \times 10^7 \left(\frac{\rho(1 - M_c/\overline{M}_n)}{M_c}\right)^{5/6} \tag{5}$$

The value of 1/2.35 for K was chosen to give best agreement with the experimental results presented in the next section. This value of K is consistent with that expected earlier since it was argued that K should be $\simeq$ ½.

The E_0A_0 average was calculated using the modulus for the crystal multiplied by the cross-sectional area per chain in the crystal, and it represents the modulus contribution of an extended chain. M_c values are available for the common materials from the reviews of Porter and Johnson,[18] Graessley,[10] and Ferry.[19] M_c values, for materials in which M_c values had not been measured, were interpolated from the plot given in Figure 4 where the molecular cross-sectional area of the polymer chain A_c was calculated[20] from

$$\text{molecular cross-sectional area} = \frac{\text{weight of repeat unit}}{(\text{sample density}) \cdot \text{length of repeat unit (i.e., } l_0)}$$

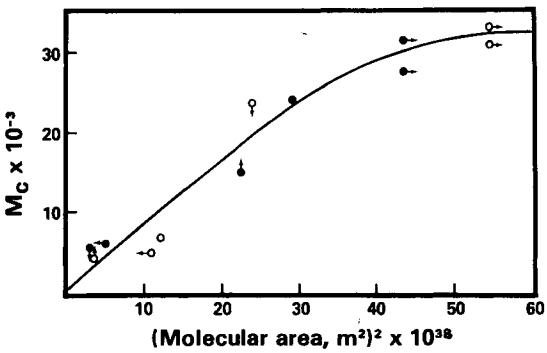

Fig. 4. Empirical plot of the critical entanglement molecular weight M_c vs. the cross-sectional area of the chain. The individual points are as follows: ⊙ polypropylene, O— polystyrene, ♀ poly(vinyl acetate), —O polycarbonate, ♁ polyethylene, ♁ polyisoprene, ● polydimethylsiloxane, ●— poly(methyl methacrylate), ♀ poly(ethylene oxide), —● 1,4 polybutadiene, and ♀ polyisobutylene.

For samples for which A_c was not previously given by Vincent,[20] the values were obtained from data as indicated by Flory.[21] For still others, l_0 was crudely calculated from the chemical structure in manner similar to that given in Figure 5. This last technique is less satisfactory than the experimental determinations, in that the calculation as given in Figure 5 should probably be taken over a number of repeat units and averaged. For example, the approximate calculation for PET as shown in Figure 5, gives a value somewhat too low as compared with the experimental value.

RESULTS AND DISCUSSION

Predictions of Breaking Stress

In the preceding section it was stated that the breaking stress under tensile impact conditions should depend little (in comparison to the yield stress) on temperature according to the LDO hypothesis. To test this point the breaking stress σ_B has been determined under tensile impact conditions (ca. 11 ft/sec being the velocity of the pendulum arm at impact) at room temperature and near liquid-nitrogen temperature for various samples that are ductile at room temperature. The exact temperature of the specimen after immersion in liquid nitrogen was not known, since in the experiment the cold sample was transferred to room-temperature grips before breaking. The transfer took 3–5 sec. The results of this study are given in Table II. All samples at low temperature were found to fail in a macroscopically brittle manner with no necking as might be inferred from Figure 6. This is to be compared to the behavior at room temperature in Figure 2. These data reinforce the earlier assumption that σ_B is primarily a function of the material. In contrast to the relatively insensitive nature of σ_B to the variation in temperature, the yield stress varied more than a factor of two between room and low temperature.

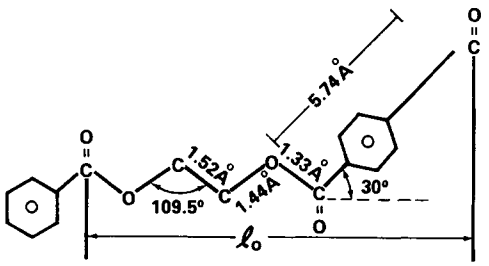

Fig. 5. Example of the calculation of the length of the repeat unit l_0 of the polymer chain. l_0 = 5.74 × cos 30° + 2 × 1.33 cos35° + 2 × 1.44 cos35° + 1.52 cos35° = 10.75 Å.

TABLE II
Effect of Yielding and Necking on Breaking Stress

Material	Ratio of low-temperature to room-temperature breaking stress
Polycarbonate (Sample A)	1.09
Poly(ethylene terephthalate) (Sample E)	1.05
Polysulfone	1.20

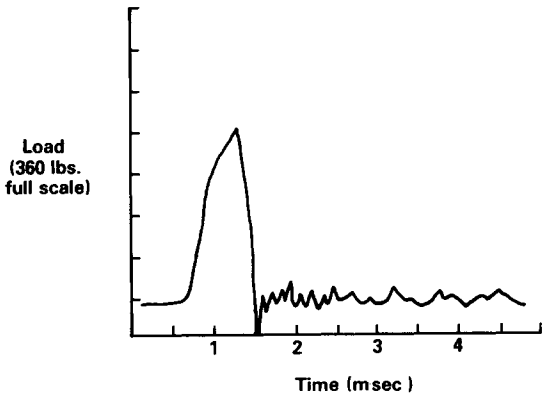

Fig. 6. Oscilloscope trace for the sample as in Figure 2, except at low temperature.

Ultrahigh-molecular-weight polyethylene (UHMWPE) has been included in this study of amorphous polymers because the UHMWPE is expected to be highly entangled like the amorphous polymers, and the crystallinity present is presumed to be of the fringed micelle type. In other words, the molecular dimensions would tend toward those of the amorphous polymer because of the difficulty in untangling due to the very high molecular weight. This aspect will be further elaborated on later.

The pertinent data to be applied to eq. (5) are given in Table I. Twice the molecular weight between entanglement points M_c has been previously shown to be estimable (Fig. 4) from the molecular cross-sectional area. The predicted and experimental breaking stresses σ_B are plotted in Figure 7. It should be noted that these breaking stresses are not based on the original cross-sectional area as is usual in reporting tensile strengths, but rather based on the cross-sectional area at break. While the correspondence between the predicted and experimental σ_B's is not in perfect agreement, the trend is unmistakable. Some of the

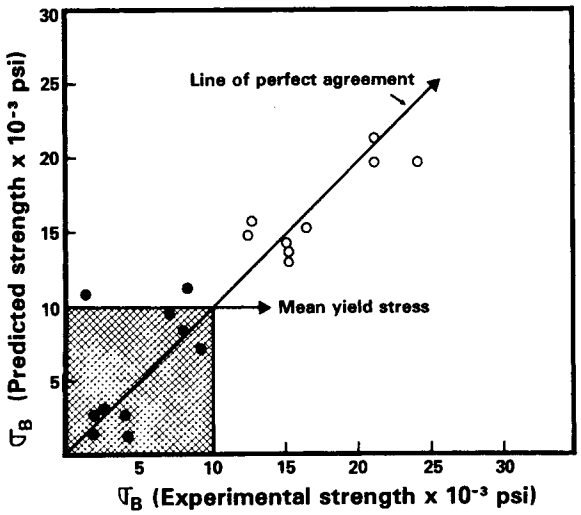

Fig. 7. Experimental stress at break vs. the stress at break as calculated from eq. (5). Cross-hatched area, brittle region, $\sigma_y \geq \sigma_B$; O ductile failure; ● brittle failure.

scatter about the line in Figure 7 probably arises from imperfect knowledge of M_c and $\overline{M}_n$, the assumption that $M_c = 2M_e$, and the crudeness of the model. Another possible reason for the scatter may be because of the implicit assumption that all connected interentanglement segments across the fracture plane carry the load equally and fracture simultaneously. It should be added that the ductile results in Table I for poly(phenylene oxide) (PPO) were for thin specimens (ca. 30 mils); tensile impact of thicker PPO specimens (ca. 80 mils) in general led to brittle fracture. The experimental data for the thin specimens is in brackets while the thick specimen data is unbracketed. Agreement seems especially poor between the predictions of the entanglement model and experimental data for the ductile break experienced in thin specimens of PPO.

For all cases the materials having an experimental σ_B greater than the average yield stress (10,000 psi for the samples listed that underwent yielding) produced a nonbrittle failure. Conversely, materials having σ_B's less than the mean yield stress (σ_y) failed in a brittle manner. This may be understood in terms of Figure 1 as follows. From average values of the flexural yield strength for poly(vinyl chloride), crystal polystyrene, polycarbonate, poly(methyl methacrylate), and polysulfone as given in the "polymer Handbook," little systematic variation in the yield strengths between the "brittle" materials such as polystyrene and the "ductile" materials such as polycarbonate is found. Therefore, the yield stresses for most of plastics studied are not substantially different. Therefore the reason why the so called brittle materials fail in a brittle manner is clear from Figures 1 and 7; the breaking stress is lower than the yield stress for the brittle materials and higher in the case of ductile failure. It was observed that, except for the UHMWPE, the standard deviation about the mean for the yield stress was only $\pm$ 1300. Consequently, due to the relatively small variation in σ_y for the samples studied here (relative to σ_B) and the observation that σ_B varies considerably in the present testing configuration, it is concluded that, *under tensile impact conditions, σ_B is the primary determinant of whether a given specimen fails in a brittle or ductile manner.* σ_B is the turn primarily determined by the entanglement density of the network. The breaking stress increases with increasing entanglement density (lower molecular weight, $M_e = M_c/2$, between entanglements).

If the above ideas are correct, then this could explain the lack of ability of dynamic mechanical spectra to clearly account for differences in ductile-brittle transitions and impact properties of amorphous one-phase polymeric systems. This is suggested by the fact that interentanglement effects are unlikely to be seen in the dynamic mechanical properties below T_g because of the relatively short chain lengths responsible for mechanical damping below T_g. This conclusion is supported by the observation by me that for poly(paramethylene benzoate), the dynamic mechanical spectra of samples H and I were found to be identical between 77 to 373°K. Samples H and I differ only in molecular weight.

While the model presented here would appear to have little in common with the widely held idea that ductility or brittleness is a direct result of chain mobility, which is in turn often thought to be relatable to mechanical transitions (glass and/or secondary), the correlation of M_c with the mass per unit length of the polymer chain suggests an indirect connection between ductility and chain mobility. The mass per unit length of polymer chain (M_0/l_0) or chain cross-

sectional area can be crudely thought of as a steric rigidity factor. Increases in chain flexability have been shown to produce[22] corresponding decreases in M_c, very much resembling the empirical relationship used here between M_c and the molecular cross-sectional area of the chain. However, no mechanism, other than the entanglement model given here, seems to explain in an obvious manner the large variations observed in breaking stress.

It is interesting to note that eq. (2) is essentially the Griffith[23] equation, in which there is present in the specimen an intrinsic flaw or crack of length $2c \equiv 1/n$. While the Griffith equation is not strictly applicable to plastic flow and cracks, in which the radius at the crack tip approaches atomic dimensions, a similar equation derived[14] on the basis of the atomic structure of materials leads to a similar relation. This relationship has been subsequently applied to an ideal glassy state. The practical link between the strength of the idealized glassy state and the real polymer (capable of plastic flow) is the key postulate in the treatment of the breaking stress as a material property.

The experimental data given in Table I for σ_B are those obtained using our instrumented impact equipment. Comparison of predictions for σ_B with the data of Vincent[20] are given in Figure 8. The data of Vincent were obtained by varying the temperature in order to pinpoint the brittle-ductile transition. Presumably, if the brittle stress varies little with temperature, these values of σ_B should be comparable with the breaking stresses of interest here. The average molecular weights of the samples examined by Vincent were sufficiently high so that further increases were reported to not affect the brittle strengths, and therefore the term $M_c/\overline{M}_n$ was considered zero for the theoretical calculations using eq. (5). While the agreement between the predictions and experimental data in Figure 8 are reasonably good for the higher brittle strength materials, the observation, that predictions for the brittle strength of the semicrystalline materials appear to agree with the experimentally determined ones as well as for the amorphous materials, is surprising. More discussion of this point will be given later.

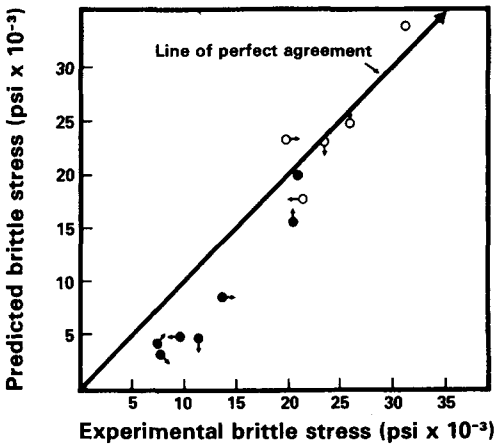

Fig. 8. Comparison of breaking stresses predicted from eq. (5) with the experimental brittle stresses as reported by Vincent (ref. 20). The individual points are ⊙ polyoxymethylene, ○ nylon, ○→ polyethylene, ○ poly(ethylene terephthalate), ←○ polysulfone, ● polycarbonate, ● poly(vinyl chloride), ●→ polypropylene, ● poly(butene-1), ←● poly(methyl methacrylate), ● polystyrene, and ● poly(methyl pentene-1).

Prediction of Tensile Impact Strength

The measured tensile impact strength should be a measure of the energy dissipated per unit of original cross-sectional area. Therefore, for ductile samples which undergo necking

$$\text{TIS} \simeq \int_{l^*}^{l} \frac{F_d\, dl}{A_0} = \frac{F_d l - F_d l^*}{A_0}$$

where F_d is the drawing load (see Fig. 2), σ_B is the breaking stress as calculated earlier, and l^* is the initial length of the sample which forms the necked region; l^* will approach zero for a brittle break. If no volume change is assumed

$$\text{TIS} = \frac{F_d l^*}{A} - \frac{F_d l^*}{A_0} = l^*(\sigma_B - \sigma_d) \tag{6}$$

For l^* in ft and σ_B and σ_d in lb./in.^{2}, the TIS is calculated to be in ft lb. in.^{2}. From Table I a trend between experimental TIS results for the ductile materials and those calculated from eq. (6) is evident. These results are also plotted in Figure 9. As can be seen from the figure, the predicted values are approximately 58% of the experimental values, although the correlation appears reasonably good. Part of the error may be in the measurement of l^*; the measurement of l^* involved considerable uncertainty since the demarcation between the necked and unnecked sections was not sharp. It should be noted that $(\sigma_B - \sigma_d)$ is the energy expended per unit volume during the tensile impact experiment.

Some Serious Difficulties

While the model presented here appears to give reasonable predictions and accounts for a number of heretofore unaccounted for phenomena, many serious difficulties remain. The model ignores the complex processes of crack growth, crack propagation, crazing and craze fracture, plastic flow, and the dynamics of fracture. By assuming that real specimens, which fail by any combination of the above failure modes, can be approximated by the failure of an idealized glassy entanglement network, it would appear that the assumption that plastic

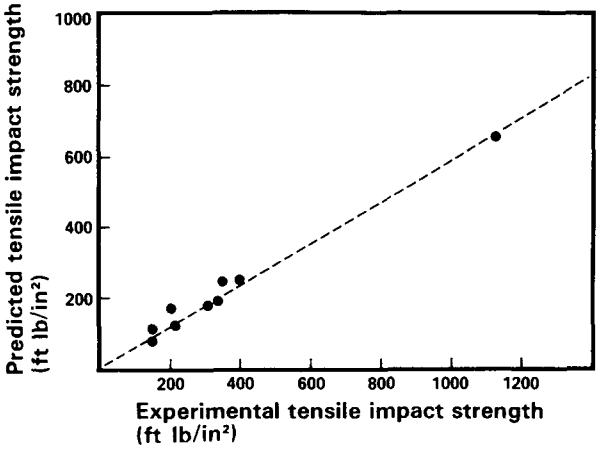

Fig. 9. Experimental tensile impact strength values vs. those calculated from eqs. (5) and (6).

flow, craze formation, and other demonstrable physical failure processes do not substantially affect the strength of the material. Of course, macroscopic flaws originally present do have a large effect as evidenced by the verification of the Griffith equation.

In the ductile real sample a neck often will form to an approximately constant cross-sectional area. Neck propagation then proceeds at constant load. Thus, for the real sample, two new aspects become important. First, the necked section is oriented, and as such, should be stronger than the isotropic network from which the calculations are made. However, as the neck propagates, older neck sections are under approximately constant stress, and as such should be less likely to survive according to the dynamics of fracture as indicated by Zhurkov's rate theory.[24] In order for my fundamental postulate to be correct, and some experimental data have been given in Table II to support it, it would appear that the effects of these two processes must cancel; a structure "strengthened" due to orientation can be made to fail at the same stress as the original structure if we allow increased time for the failure to occur. More work in this area is necessary to more convincingly demonstrate the physical reality of this postulate.

The value of l^* in eq. (6) is of critical importance for predicting tensile impact strength. At present no systematic way of predicting it is known to this author. However, my experience to date generally indicates that l^* tends to increase with breaking stress, although l^* varies with molding conditions. Work is continuing on this aspect of tensile impact strength and the results will be presented in a future publication.

The agreement between the predicted and experimental breaking strengths for both amorphous and polycrystalline polymers of high molecular weight is, at first glance, surprising. However, neutron scattering experiments discussed by Flory and Yoon[25] have shown that a molecule of polyethylene has essentially the same radius of gyration in the melt as in the bulk crystallized state. These results indicate that for the crystalline state, relatively high-molecular-weight polymers are entangled much like the melt or amorphous state. In other words, entanglements are not lost during crystallization. In terms of strength, crystallites might be considered multifunctional crosslinks, but for $\sigma_B \gg \sigma_y$ these crosslinks would probably not contribute measurably to the strength since they would be destroyed under stresses exceeding the yield stress.

CONCLUSIONS

The agreement of the model with the experimental results leads to the following conclusions. Under the tensile test conditions used here, whether a given amorphous material fails in a brittle manner (usually leading to poor impact strength) or in a ductile fashion, depends chiefly on the intrinsic strength of the material in tension, which is postulated to be dependent on the entanglement network density. The entanglement density is, in turn, dependent on number-average molecular weight and the mass per length of the molecular chain (proportional to the molecular cross-sectional area).

If the entanglement model presented here is correct, difficulties in relating dynamic mechanical properties below T_g to breaking stress and tensile impact properties of amorphous polymers are understandable because below T_g the

dynamic mechanical properties mirror relaxation mechanisms of chain segments considerably smaller than the interentanglement spacings.

References

1. E. Orowan, *Rept. Prog. Phys.*, **12**, 185 (1949).
2. L. Bohn and H. Oberst, *Acustica*, **9**, 431 (1959).
3. J. A. Sauer, *J. Polym. Sci. Polym. Symp.*, **32**, 69 (1971).
4. G. S. Yeh and M. Wyzoski, *J. Macromol. Sci., Phys.* **B 10**(3), 441 (1974).
5. R. F. Boyer, *Polym. Eng. Sci.*, **8**, 161 (1968).
6. F. Bueche, B. Kinzig, and C. Coven, *J. Polym. Sci. Polym. Lett. Ed.*, **3**, 399 (1965).
7. B. Murphy, R. Howard, and E. White, *J. Polym. Sci., A-2*, **9**, 801 (1971).
8. R. N. Haward, *The Physics of Glassy Polymers*, Wiley, Toronto, 1973, Chap. 5.
9. J. P. Berry, *Fracture Processes in Polymeric Solids*, R. Roesen, Ed., Interscience, New York, 1964, Chap. IIB.
10. W. W. Graessley, *Advances in Polymer Science*, Vol. 16, Springer-Verlag, New York, 1974, p. 55.
11. P. I. Vincent, *Polymer*, **1**, 425 (1960).
12. J. P. Berry, *J. Polym. Sci., A* **1**, 993 (1963).
13. F. Bueche, *Physical Properties of Polymers*, Interscience, New York, 1962, p. 237.
14. E. Orowan, *Weld. J. Res. Suppl.*, **34**, 157-S (1955).
15. E. Orowan, *Trans. Inst. Eng. Shipbuild. Scotl.*, **89**, 165 (1946).
16. F. Daniels and R. Alberty, *Physical Chemistry*, Wiley, New York, 1961, p. 73.
17. I. Sakurada, T. Ito, and K. Nakamae, *J. Polym. Sci., Part C*, **15**, 75 (1966).
18. R. Porter and J. Johnson, *Chem. Rev.*, **66**(1), 1 (1966).
19. J. D. Ferry, *Viscoelastic Properties of Polymers*, Wiley, 1970, p. 409.
20. P. I. Vincent, *Polymer*, **13**, 558 (1972).
21. P. J. Flory, *Statistical Mechanics of Chain Molecules*, Interscience, New York, 1969.
22. C. Beatty, *Am. Chem. Soc. Polym. Prepr.*, 344 (1977), especially Polymer Coatings Section, p. 344.
23. A. Griffith, *Philos. Trans. R. Soc.*, **221**, 163 (1921).
24. S. Zhurkov, *Int. J. Fracture Mech.*, **11**, 5 (1975).
25. P. Flory and D. Yoon, *Nature*, **272**, 226 (1978).

Received June 29, 1978
Revised October 23, 1978